Contents lists available at ScienceDirect

New BIOTECHNOLOGY

journal homepage: www.elsevier.com/locate/nbt

Full length Article

FN3-based monobodies selective for the receptor binding domain of the SARS-CoV-2 spike protein

Christina J. Miller [a], Jennifer E. McGinnis [a], Michael J. Martinez [a], Guangli Wang [b], Jian Zhou [c], Erica Simmons [d], Tohti Amet [d], Sanofar J. Abdeen [d], James W. Van Huysse [d], Ronald R. Bowsher [d], Brian K. Kay [a],*

[a] *Tango Biosciences, Inc., 2201 W. Campbell Park Drive, Chicago, IL 60612 USA*
[b] *Euprotein Inc., 675 US Highway 1, Suite 129, North Brunswick, NJ 08902 USA*
[c] *LifeTein LLC, 100 Randolph Road, Suite 2D, Somerset, NJ 08873 USA*
[d] *B2S Life Sciences, 97 East Monroe Street, Franklin, IN 46131 USA*

ABSTRACT

A phage library displaying 10^{10} variants of the fibronectin type III (FN3) domain was affinity selected with the biotinylated form of the receptor binding domain (RBD, residues 319–541) of the SARS-CoV-2 virus spike protein. Nine binding FN3 variants (i.e. monobodies) were recovered, representing four different primary structures. Soluble forms of the monobodies bound to several different preparations of the RBD and the S1 spike subunit, with affinities ranging from 3 to 14 nM as measured by bio-layer interferometry. Three of the four monobodies bound selectively to the RBD of SARS-CoV-2, with the fourth monobody showing slight cross-reactivity to the RBD of SARS-CoV-1 virus. Examination of binding to the spike fragments and its trimeric form revealed that the monobodies recognise at least three overlapping epitopes on the RBD of SARS-CoV-2. While pairwise tests failed to identify a monobody pair that could bind simultaneously to the RBD, one monobody could simultaneously bind to the RBD with the ectodomain of the cellular receptor angiotensin converting enzyme 2 (ACE2). All four monobodies successfully bound the RBD after overexpression in Chinese hamster ovary (CHO) cells as fusions to the Fc domain of human IgG1.

Introduction

The current Coronavirus-Disease-2019 pandemic (COVID-19) caused by Severe Acute Respiratory Syndrome coronavirus 2 (SARS-CoV-2) is a respiratory disease that has led to millions of infections and deaths worldwide [1]. This outbreak marks the third coronavirus causing large-scale threat and harm to the population in the 21st century, after the Severe Acute Respiratory Syndrome coronavirus (SARS-CoV) in 2002 and the Middle East Respiratory Syndrome coronavirus (MER-S-CoV) in 2012. Like SARS and MERS, viral infection with SARS-CoV-2 can lead to Acute Respiratory Distress Syndrome, with potentially long-term reduction in lung function, heart arrhythmia, and death [2–4]. However, COVID-19 has shown a much greater propensity for infectivity relative to SARS and MERS, which has made the current global pandemic more difficult to contain.

Each SARS-CoV-2 viral particle consists of a lipid membrane envelope that is decorated with spike (S), membrane (M), and envelope (E) proteins, and carries a 30 kb single-stranded RNA and nucleocapsid (N) protein [5–7]. The biomedical research community has targeted the S glycoprotein in diagnostic assays and antiviral therapies, as it is abundant, accessible, and plays a crucial role in viral entry into host cells. Upon viral infection, the trimeric S protein is cleaved into its two subunits, S1 and S2; the S1 subunit carries the Receptor Binding Domain (RBD), and the S2 subunit fuses with the host membrane. The RBD binds to the human angiotensin converting enzyme-2 (ACE2) of respiratory epithelial cells, directing cellular uptake by endocytosis [8,9]. The three-dimensional structure of the SARS-CoV-2 RBD complexed to ACE2 has been solved [10–13].

Rapid diagnostic tests and antiviral therapeutics that utilize antibodies to detect viral particles and block viral receptors, respectively, have become extremely useful in combatting many viruses [14,15]. However, generating such high-quality antibodies that can bind these proteins with high affinity and specificity is time consuming and challenging. With advances in various display technologies [16–22], recombinant antibodies and antibody surrogates are faster to generate than conventional antibodies through animal immunization. Thus, recombinant affinity reagents can include alternative, non-antibody-based scaffolds that circumvent the limitations of traditional antibodies [18]. The Fibronectin Type III (FN3) domain, derived from the 10th domain of human fibronectin, has been engineered to bind to a wide variety of human proteins [23–28].

Several FN3 reagents, known as monobodies, have either reached clinical trial or shown promising results as diagnostic tools [29–32]. Here, the isolation of monobodies binding to the receptor binding domain (RBD) of SARS-CoV-2 is reported. A phage library displaying 10^{10} monobody variants was used in affinity selection with a biotinylated fusion protein consisting of the C-terminus of a 222 amino acid segment containing the spike RBD attached to the Fc region of human IgG1. Four different monobodies were recovered and demonstrated to bind with high affinity and specificity to the RBD. We envisage that these engineered monobodies can be further developed into tools for diagnostic assays.

Materials & methods

Preparation of SARS-CoV-2 viral spike and cellular receptor proteins

Expi293 F cells (ThermoFisher, Waltham, MA), grown in shaker flasks, were transfected with expression plasmids harbouring synthetic genes encoding the Fc region of human IgG1 (E99-K330), fused to the SARS-CoV-2 spike RBD (RBD-Fc) and human ACE2 ectodomains (ACE2-Fc), as well as the human IgG1 Fc region alone. The RBD and ACE2 ectodomains correspond to residues 319–541 of the SARS-CoV-2 spike protein and 18–708 of ACE2, respectively. Plasmid DNA was mixed with ExpiFectamine™ 293 reagent (ThermoFisher) and Opti-MEM medium (ThermoFisher) in an optimized ratio for transient transfection. Four to 5 days after transfection, the conditioned cell culture was harvested by centrifugation at $4500 \times g$ for 10 min. The clarified supernatant was collected and diluted with equal volume of binding buffer (20 mM Na_2HPO_4, 150 mM NaCl, pH 7.4), and loaded onto a Protein A chromatography column (GE Healthcare Life Sciences, Marlborough, MA) followed by washing with 20 column volumes (CV) of binding buffer. The bound IgG fusion proteins were eluted from the column with 5–10 CV of 0.2 M glycine, pH 2 elution buffer. After dialysis with phosphate buffered saline (PBS; 137 mM NaCl, 3 mM KCl, 8 mM Na_2HPO_4, 1.5 mM KH_2PO_4), the purified protein was characterized by sodium dodecyl sulfate-polyacrylamide gel electrophoresis (SDS-PAGE) in a 4 %–12 % Bis-Tris gel (ThermoFisher) in running buffer (50 mM 3-morpholinopropane-1-sulfonic acid, 50 mM Tris base, 0.1 % SDS, 1 mM EDTA, pH 7.7). The protein concentration was determined with the bicinchoninic acid assay (ThermoFisher). Aliquots of the RBD-Fc protein and an unrelated IgG1 Fc fusion to a 33 amino acid segment (Fc-peptide) of human CD24 were chemically biotinylated via EZ-Link™ Sulfo-NHS-LC-Biotin (ThermoFisher). An aliquot of the ACE2 ectodomain-Fc protein was conjugated to horseradish peroxidase (HRP) with the HRP Lightning-Link kit (Abcam, Cambridge, UK), according to the manufacturer's instructions.

A plasmid (pCAGGS-SARS-CoV-2-Wuhan-Hu-1 Spike), containing an open reading frame encoding a nearly full-length SARS-CoV-2 spike protein, was obtained from the laboratory of Dr. Florian Krammer (Department of Microbiology at the Icahn School of Medicine at Mount Sinai, NY, New York) via the Biodefense and Emerging Infections Research Resources Repository. The C-terminal transmembrane spanning domain of the spike protein sequence was omitted to create a

soluble form of the protein [1]. Residues 986 and 987 were mutated to proline [33], which lock the spike trimer in the active (prefusion) conformation for viral attachment to the host receptor, ACE2.

A His6-tag was added to the spike protein C-terminus. The trimeric version of the SARS-CoV-2 spike protein was expressed by culture and transient transfection of Expi293 F cells (ThermoFisher), as described elsewhere [34], and purified by chromatography over Ni-nitrilotriacetic acid agarose (Qiagen, Hilden, Germany). Size-exclusion chromatography of the protein preparation demonstrated that the major absorbance peak resolved with the expected molecular weight of a trimeric complex (670 kDa).

Commercial sources of SARS-CoV-2 spike protein were also used in various experiments: His6-tagged RBD preparations were from Sino Biologics (Beijing, China) and RayBiotech Life (Peachtree Corners, GA, USA) and His6-tagged S1 spike protein was from SignalChem Biotech (Richmond, BC, Canada). A human monoclonal antibody, CR3022 [35], to the spike protein of SARS-CoV-2 virus was purchased from InvivoGen (San Diego, CA).

Affinity selection

An M13 bacteriophage library, displaying FN3 monobodies [36] at the N-terminus of truncated protein III (aa 257–406), was affinity selected with chemically biotinylated RBD-Fc fusion protein, following previously described protocols [37]. After two rounds, 96 clones were examined for binding by enzyme linked immunosorbent assay (ELISA), as previously described [37], and the DNA inserts of 9 clones that bound the RBD-Fc fusion protein, but not the Fc-peptide fusion protein (negative control), were sequenced by Sanger dideoxy sequencing at the Sequencing Core at the Research Resources Center at the University of Illinois at Chicago.

Subcloning and purification of soluble forms of four monobodies

For overexpression in *Escherichia coli*, the FN3 coding regions were amplified by PCR from phage clones and subcloned into the pMAL-c6T vector (New England BioLabs, Ipswich, MA). The vector included a His6-tag for purification [38] and the maltose-binding protein (MBP) N-terminal to the monobody for improved bacterial expression [39]. MBP-FN3 fusion proteins were overexpressed and purified according to the manufacturer's directions.

To construct FN3-Fc fusions, the monobody coding regions were inserted into the vector pGen2 (DNASU, Tempe, AZ) downstream of the signal sequence for lysosomal α-mannosidase, followed by a $(GGGGS)_2$ linker, the Fc coding region for human IgG1, and the sortase recognition motif, LPETG. Culturing of transfected Chinese Hamster Ovary (CHO) cells (ThermoFisher) and purification of the secreted Fc fusion proteins followed the methods above.

Enzyme linked immunosorbent assay (ELISA)

The general format of the ELISA assay is described below with specifics reported in the individual figure legends. Proteins were diluted in 0.1 M NaHCO₃ and added at a fixed or range of concentrations to Nunc Maxisorp™ flat-bottom 96 well plates (ThermoFisher), at 100 µL per well, in triplicate. After incubation at room temperature for 45 min, the wells were washed once in PBS-0.1 % Tween 20 (PBST), and non-specific binding sites on the plate surface were blocked with 5% skim milk in 0.1 M NaHCO₃ for 30 min. The wells were then washed once in PBST, and proteins under study were added at a fixed or increasing concentrations to the wells.

After 45 min incubation, the wells were washed 3x in PBST before adding streptavidin-horseradish peroxidase conjugate (HRP; Sigma-Aldrich, St. Louis, MO), anti-human IgG-HRP (Abcam) or ACE2-Fc-HRP (see above) to the wells for 1 h incubation. After washing the wells 3x in PBST, 100 µL of 2',2'-Azino-Bis 3-Ethylbenzothiazoline-6-

Sortase-mediated ligation

The purified FN3A-Fc fusion protein (12 μM), which carried a C-terminal sortase tag, was incubated with 1 unit of Sortase A5 enzyme (Active Motif, Carlsbad, CA) and 25 μM of N terminal (Glycine)$_5$-HRP protein (Active Motif) for 1 h at 30 °C. The ligation reactions were then buffer exchanged with 50 kDa molecular weight cut-off, Amicon® Ultra Centrifugal Filters (MilliporeSigma, Burlington, MA) at ~ 1500 × g for 10 min to remove unconjugated HRP.

Results & discussion

Generation of recombinant spike and cellular receptor proteins

To develop recombinant affinity reagents to the SARS-CoV-2 virus, the receptor binding domain (RBD) of the spike protein was targeted for affinity screening via phage display. The RBD was successfully overexpressed in Expi293 F cells as a fusion to human IgG1 Fc. After the Protein A-purified sample was resolved under reducing conditions by SDS-PAGE, the RBD-Fc fusion migrated as expected as a ~65 kDa species (Fig. 1a). The ectodomain of human ACE2 was overexpressed as an Fc fusion protein and purified in the same manner as the RBD fusion protein. The observed molecular weight of the ACE2-Fc fusion product was ~ 110 kDa, which was larger than anticipated and likely due to post-translational glycosylation (Fig. 1b). The RBD-Fc fusion protein was chemically biotinylated and utilized as a target in phage-display experiments.

To assess the binding properties of monobodies isolated by phage display, the spike trimer was also prepared. The spike protein of coronavirus trimerizes due to a C-terminal T4 fibritin trimerization domain [40]. Amino acids 1–1255 of the SARS-CoV-2 virus spike protein were expressed in Expi293 F cells in culture (Fig. 1c). The trimer was first examined for recognition by commercial sera from COVID-19 positive patients. As seen in Suppl. Fig. S1, the preparation of spike protein produced an excellent signal response when coated passively on an ELISA plate and probed with serum samples with known positivity for SARS-CoV-2. The observed signal responses demonstrated efficient competitive inhibition upon preincubation with 5 mg/mL of trimer protein (Suppl. Fig. S2). In contrast, a sample from a normal healthy adult failed to produce a signal response above background (Suppl. Fig. S2). Finally, Suppl. Fig. S3 shows that the ACE2-Fc fusion, chemically conjugated to HRP, binds well to the SARS-CoV-2 virus RBD and spike trimer, indicating that the RBD is accessible in the spike trimer preparation.

Affinity selection of monobodies that bind the RBD of SARS-CoV-2

A library of M13 bacteriophage virions, displaying 10^{10} variants of the FN3 monobody [36], was screened by affinity selection with the biotinylated RBD-Fc fusion captured by streptavidin-coated beads. The coding regions of the BC, DE, and FG loops (Fig. 2a) in the library were randomized with variable lengths of triplet codons encoding 30 % TYR, 15 % SER, 15 % GLY, 5% THR and PHE, and 2.3 % all other residues, excluding CYS and MET. After two rounds of affinity selection, output clones were examined for binding by ELISA. As shown in Fig. 2b, four different FN3 binders were identified that bound the RBD-Fc fusion protein and not the Fc-peptide protein. The complete primary structures of the FN3 variants, referred to as FN3A-D, are aligned in Suppl. Fig. S4. When comparing the amino acid composition of the loop regions, the binders appeared to favor a high frequency of tyrosine residues (Fig. 2c), corroborating numerous reports of high tyrosine content in the complementarity determining regions of antibodies [41–44]. It was confirmed by ELISA that the four phage-display clones could bind other preparations of the RBD such as His$_6$-tagged RBD and the S1 subunit (Suppl. Fig. S5).
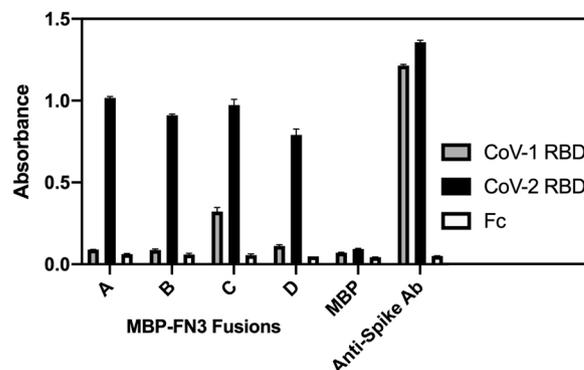
Fig. 3. Specificity of anti-RBD monobodies. The four MBP-FN3 fusions were adsorbed on microtiter plate wells and incubated with chemically biotinylated SARS-CoV-1 and SARS-CoV-2 RBD proteins mixed with a bacterial cell lysate. Wells coated with MBP alone served as a negative control and wells coated with an anti-spike monoclonal antibody, clone CR3022 [35], which binds equally well to the RBDs of both SARS-CoV-1 and SARS-CoV-2, served as a positive control. Binding of SARS-CoV-1 and SARS-CoV-2 RBD-Fc fusion proteins was revealed with streptavidin-HRP. Error bars represent standard error (SE) of triplicate measurements.

Characterization of the binding properties of the anti-RBD monobodies

To work with soluble forms of the four monobodies, their coding regions were subcloned into an expression vector to yield MBP fusions with an N-terminal His$_6$-tag. The recombinant MBP-FN3 fusion proteins were overexpressed in *E. coli* and purified by IMAC. To assess their specificity, ELISA was performed with the RBDs of the SARS-CoV-1 and SARS-CoV-2 viruses, which share 85 % sequence identity. The small degree of variation has been thought to explain the tighter binding of the SARS-CoV-2 to ACE2 when compared to SARS-CoV-1 [45,46]. Wells were coated with either His$_6$-tagged RBD of each virus or with Fc alone, and then probed individually with biotinylated MBP-FN3 fusions and streptavidin-HRP. A commercially available anti-spike monoclonal antibody that bound equally well to the RBD of both viruses served as a positive control. FN3A, FN3B, and FN3D bound selectively to the RBD of SARS-CoV-2, while FN3C cross-reacted partially with the RBD of SARS-CoV-1 (Fig. 3). Thus, FN3A, FN3B, and FN3D were determined to be selective for the RBD of SARS-CoV-2 virus, warranting testing against additional betacoronaviruses [47].

Fig. 4a shows the binding patterns of the four MBP-FN3 fusions to the RBD-Fc fusion and spike trimer. All four bound to the RBD-Fc fusion and not to the negative control Fc protein. Interestingly, FN3A, FN3B, and FN3D bound to the spike trimer, whereas FN3C did not, indicating that the epitopes recognized by FN3A, FN3B, and FN3D are accessible in the assembled trimer, whereas the epitope recognized by FN3C is not (Fig. 4b). No binding was observed for the four FN3s to the Fc-peptide fusion protein (Fig. 4c).

The binding kinetics of FN3A-D for the RBD of SARS-CoV-2 were evaluated by BLI. The RBD domain was immobilized on the surface of amine reactive biosensors that were incubated in parallel with a range of concentrations of the four FN3-MBP fusions, along with MBP alone (negative control). The binding data best fit a 1:1 model of protein-protein interaction. Table 1 reports the k_{on} and k_{off} rates, as well as calculated K$_D$ values. The equilibrium dissociation constants ranged from 3 to 14 nM, which is comparable to what has been observed for FN3 binders to various targets [48].

We next investigated if pairings of the monobodies could form a "sandwich" and both bind simultaneously with the RBD. None of the 6 possible pairwise combinations were observed to form a sandwich with the RBD, suggesting that the monobodies bound to either the same or
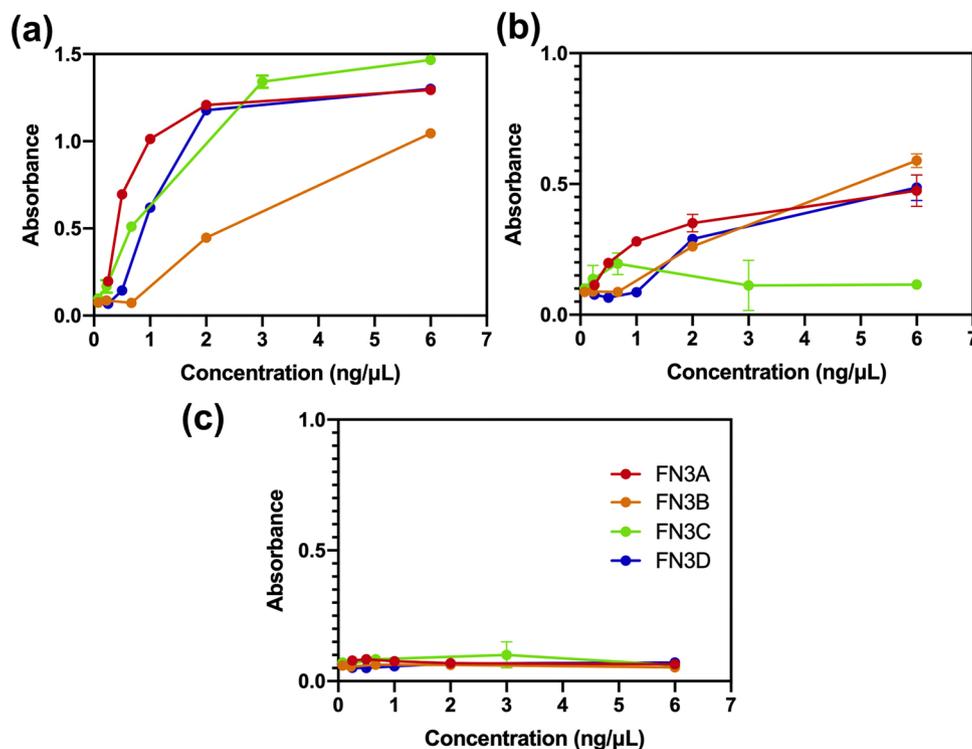
Fig. 4. Binding profiles of the four MBP-FN3 fusions. The four monobodies were expressed as MBP fusions and tested across a range of concentrations (0.07 ng/μL – 6.0 ng/μL) to assess binding to RBD-Fc **(a)** and the spike trimer **(b)** protein preparations. In the ELISA, wells were coated with RBD-Fc, Fc-peptide, and spike trimer and then incubated with biotinylated MBP-FN3 fusions or MBP alone; binding of the biotinylated proteins was revealed with streptavidin-HRP. The Fc-peptide fusion protein was used as a negative control **(c)**. Error bars represent SE of triplicate measurements.

Table 1

Binding kinetic constants and associated errors for MBP fusions and MBP alone binding to the RBD of SARS-CoV-2.

	k_{on} (1/M*s x 10^4)	k_{off} (1/s x 10^{-4})	R^2	K$_D$ (nM)
MBP-FN3A	7.60	4.23	0.992	5.56 ± 0.15
MBP-FN3B	6.42	3.68	0.992	5.73 ± 0.21
MBP-FN3C	4.03	5.63	0.972	14.00 ± 0.26
MBP-FN3D	2.35	0.80	0.995	3.41 ± 0.43
MBP alone	n.d.[†]	n.d.[†]	n.d.[†]	n.d.[†]

The calculated kinetic parameters for the interaction between the individual MBP-FN3 fusions and the RBD protein. The data were fit by the Octet HTX Analysis Software version 11.0 with a 1:1 binding model to generate the k_{on}, k_{off}, and K$_D$ values (association and dissociation rate constants, and equilibrium dissociation constant, respectively).

[†] No specific binding was observed between the RBD protein and MBP alone; therefore, no kinetics parameters were calculated for this interaction.

overlapping epitopes on the RBD surface. However, it was observed that FN3A could form a sandwich with ACE2-Fc and the RBD-Fc (Fig. 5), with a half maximal effective concentration (EC$_{50}$) of 57 nM. It should be noted that the FN3A-RBD-ACE2 complex could form in the presence of excess *E. coli* cellular proteins, indicative of high specificity for FN3A and ACE2 binding the SARS-CoV-2 virus RBD.

Examination of the 3D structural determination of the RBD-ACE2 complex [13] indicates that sufficient room exists for the 94–97 amino acid long monobodies to potentially bind the RBD away from its ACE2 binding surface (Suppl. Fig. S6). Several neutralizing antibodies have recently been demonstrated to bind outside the ACE2 site [49]. In order to identify a monobody that blocks the interaction between the RBD and ACE2, competitive elution may be required during the affinity selection
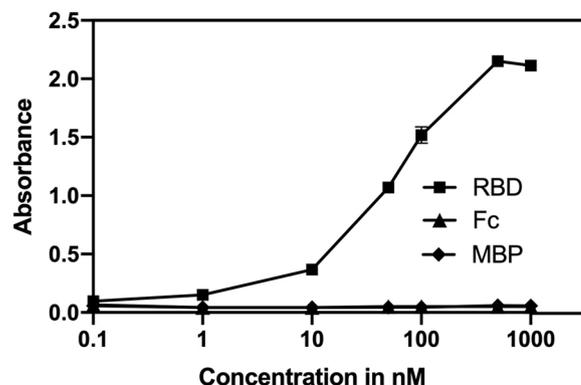
Fig. 5. Detection of the SARS-CoV-2 RBD in a complex biological mixture. An *E. coli* cell lysate was mixed with various concentrations of SARS-CoV-2 RBD and added to microtiter wells coated with the FN3A-MBP fusion protein. After incubation and washing of the wells, the ectodomain of ACE2, conjugated to HRP, was added. Negative controls consisted of MBP *in lieu* of FN3A and Fc alone *in lieu* of RBD. Error bars represent SE of triplicate measurements.

process [50].

Based on characterization of the four monobodies, we infer that they bind to at least three overlapping epitopes on the RBD of SARS-CoV-2. FN3A is the only one that can bind the RBD and still allow ACE2 binding, FN3C is the only one that fails to bind the RBD in the spike trimer preparation, and FN3B and FN3D bind differently than FN3A and FN3C.
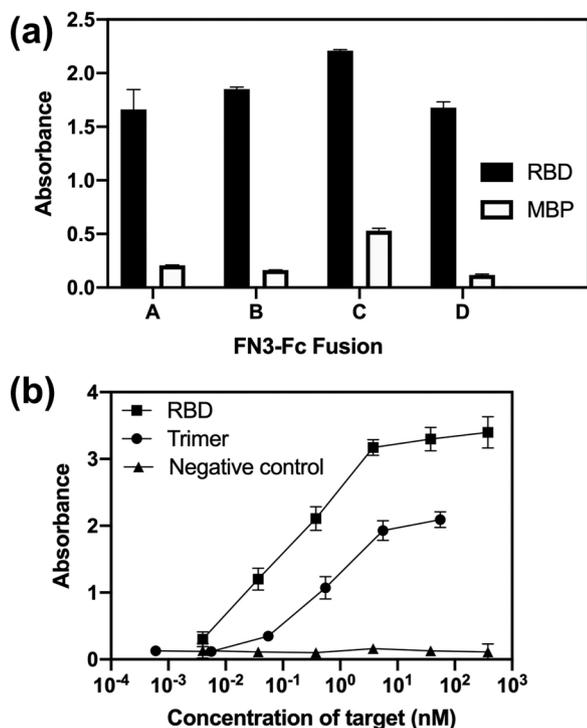
Fig. 6. FN3-Fc fusions bind to the RBD. (a) Confirmation of functional FN3-Fc fusions by ELISA. Microtiter wells were coated directly with RBD or MBP, incubated with the individual FN3-Fc fusions, and then probed with anti-IgG-HRP antibodies. Error bars represent SE of triplicate measurements. (b) Soluble RBD (non-Fc fusion; Sino Biological), trimer, and MBP (negative control) were immobilized in microtiter wells over a range of concentrations and probed with the FN3A-Fc fusion sortase-ligated to HRP. Error bars represent SE of triplicate measurements.

Additional experiments are warranted to map the epitopes recognized by the monobodies more precisely.

These findings corroborate the report that recombinant antibodies can be engineered to recognize multiple epitopes on the RBD [51–53]. Additionally, a sandwich assay to detect virus particles in complex biological mixtures can be created with FN3A and the ACE2 ectodomain or a surrogate [54]. As diagnostic assays in clinics typically utilize antibodies, the four monobodies were reformatted as Fc fusion proteins. The coding regions were inserted into a vector that encoded the CH2 and CH3 regions of IgG1 and a C-terminal sortase-tag (Suppl. Fig. S7), and transiently transfected into CHO cells. All four purified FN3-Fc fusions bound well to the His_6-tagged RBD, as detected with an anti-IgG-HRP antibody conjugate (Fig. 6a). Sortase [55–57] was used to ligate the Fc fusion to HRP for functional testing in an ELISA. As seen in Fig. 6b, the sortase-tagged FN3A-Fc fusion bound in a concentration dependent manner to immobilized RBD-Fc protein and spike trimer.

While these initial results for four monobodies are promising with respect to their potential as reagents in clinical assays, it will be important to verify their functional utility in the creation of reliable analytical methods (i.e., wide dynamic range, high sensitivity and specificity) with either saliva [58] or nasopharyngeal lavages [59] from COVID-19 infected individuals. By creating a secondary phage library through error-prone PCR and including more stringent conditions within the selection process, their affinity, specificity, and thermal stability can be improved [60]. For example, it is possible to engineer monobodies with pM affinities [61]. Monobodies can also be engineered to contain unnatural amino acids through stop-codon suppression [62] or fused to protein complementation systems [63]. These monobodies,

and other recombinant affinity reagents generated through phage- and ribosome-display technologies [50,52,64,65], have the potential to play a role in diagnosis of COVID-19 patients. In conclusion, the reagents created herein represent tools that can be developed further in the fight to combat the current pandemic.

Appendix A. Supplementary data

Supplementary material related to this article can be found, in the online version, at doi:https://doi.org/10.1016/j.nbt.2021.01.010.

References

[1] Worldmeters.info, Covid-19 pandemic. 2020. https://www,worldmeters.info/coronovirus/.
[2] Batah SS, Fabro AT. Pulmonary pathology of ARDS in COVID-19: a pathological review for clinicians. Respir Med 2020;176:106239.
[3] Trypsteen W, Van Cleemput J, Snippenberg WV, Gerlo S, Vandekerckhove L. On the whereabouts of SARS-CoV-2 in the human body: a systematic review. Pathog 2020;16(10). e1009037.
[4] Vakili K, Fathi M, Pezeshgi A, Mohamadkhani A, Hajiesmaeili M, et al. Critical complications of COVID-19: a descriptive meta-analysis study. Rev Cardiovasc Med 2020;21(3):433–42.
[5] Bar-On YM, Flamholz A, Phillips R, Milo R. SARS-CoV-2 (COVID-19) by the numbers. Elife 2020;9. e57309.
[6] Ke Z, Oton J, Qu K, Cortese M, Zila V, McKeane L, et al. Structures and distributions of SARS CoV-2 spike proteins on intact virions. Nature 2020;588(7838):498–502.
[7] Yu A, Pak AJ, He P, Monje-Galvan V, Casalino L, et al. A multiscale coarse-grained model of the SARS-CoV-2 virion. Biophys J 2020. https://doi.org/10.1016/j.bpj.2020.10.048.
[8] Hoffmann M, Kleine-Weber H, Schroeder S, Kruger N, Herrler T, et al. SARS-CoV-2 cell entry depends on ACE2 and TMPRSS2 and is blocked by a clinically proven protease inhibitor. Cell 2020;181(2):271–80. e8.
[9] Ou X, Liu Y, Lei X, Li P, Mi D, Ren L, et al. Characterization of spike glycoprotein of SARS-CoV-2 on virus entry and its immune cross-reactivity with SARS-CoV. Nat Commun 2020;11(1):1620.
[10] Chen Y, Guo Y, Pan Y, Zhao ZJ. Structure analysis of the receptor binding of 2019-nCoV. Biochem Biophys Res Commun 2020;525(1):135–40.
[11] Lan J, Ge J, Yu J, Shan S, Zhou H, Fan S, et al. Structure of the SARS-CoV-2 spike receptor-binding domain bound to the ACE2 receptor. Nature 2020;581(7807):215–20.
[12] Shang J, Ye G, Shi K, Wan Y, Luo C, Aihara H, et al. Structural basis of receptor recognition by SARS-CoV-2. Nature 2020;581(7807):221–4.
[13] Yan R, Zhang Y, Li Y, Xia L, Guo Y, Zhou Q. Structural basis for the recognition of SARS-CoV-2 by full-length human ACE2. Science 2020;367(6485):1444–8.
[14] Grandien M. Viral diagnosis by antigen detection techniques. Clin Diagn Virol 1996;5(2-3):81–90.
[15] Lu RM, Hwang YC, Liu IJ, Lee CC, Tsai HZ, Li HJ, et al. Development of therapeutic antibodies for the treatment of diseases. J Biomed Sci 2020;27(1):1.
[16] Mondon P, Dubreuil O, Bouayadi K, Kharrat H. Human antibody libraries: a race to engineer and explore a larger diversity. Front Biosci 2008;13:1117–29.
[17] Cherf GM, Cochran JR. Applications of yeast surface display for protein engineering. Methods Mol Biol 2015;1319:155–75.
[18] Bradbury A, Pluckthun A. Reproducibility: standardize antibodies used in research. Nature 2015;518(7537):27–9.
[19] Salema V, Fernandez LA. Escherichia coli surface display for the selection of nanobodies. Microb Biotechnol 2017;10:1468–84. https://doi.org/10.1111/1751-7915.12819.
[20] Ledsgaard L, Kilstrup M, Karatt-Vellatt A, McCafferty J, Laustsen AH. Basics of antibody phage display technology. Toxins (Basel) 2018;10(6):236.
[21] Gray A, Bradbury ARM, Knappik A, Pluckthun A, Borrebaeck CAK, Dubel S. Animal-free alternatives and the antibody iceberg. Nat Biotechnol 2020;38(11):1234–9.
[22] Kunamneni A, Ogaugwu C, Bradfute S, Durvasula R. Ribosome display technology: applications in disease diagnosis and control. Antibodies (Basel) 2020;9(3):28.
[23] Huang R, Fang P, Kay BK. Isolation of monobodies that bind specifically to the SH3 domain of the Fyn tyrosine protein kinase. N Biotechnol 2012;29(5):526–33.

[24] Huang R, Gorman KT, Vinci CR, Dobrovetsky E, Graslund S, Kay BK. Streamlining the pipeline for generation of recombinant affinity reagents by integrating the affinity maturation step. Int J Mol Sci 2015;16(10):23587–603.

[25] Park SH, Park S, Kim DY, Pyo A, Kimura RH, Sathirachinda A, et al. Isolation and characterization of a monobody with a fibronectin domain III scaffold that specifically binds EphA2. PLoS One 2015;10(7). e0132976.

[26] Richards J, Miller M, Abend J, Koide A, Koide S, Dewhurst S. Engineered fibronectin type III domain with a RGDWXE sequence binds with enhanced affinity and specificity to human alphavbeta3 integrin. J Mol Biol 2003;326(5):1475–88.

[27] Wojcik J, Hantschel O, Grebien F, Kaupe I, Bennett KL, Barkinge J, et al. A potent and highly specific FN3 monobody inhibitor of the Abl SH2 domain. Nat Struct Mol Biol 2010;17(4):519–27.

[28] Yeh JT, Binari R, Gocha T, Dasgupta R, Perrimon N. PAPTi: a peptide aptamer interference toolkit for perturbation of protein-protein interaction networks. Sci Rep 2013;3:1156.

[29] Bloom L, Calabro V. FN3: a new protein scaffold reaches the clinic. Drug Discov Today 2009;14(19-20):949–55.

[30] Natarajan A, Patel CB, Ramakrishnan S, Panesar PS, Long SR, Gambhir SS. A novel engineered small protein for positron emission tomography imaging o human programmed death ligand-1: validation in mouse models and human cancer tissues. Clin Cancer Res 2019;25(6):1774–85.

[31] Sirois AR, Deny DA, Baierl SR, George KS, Moore SJ. Fn3 proteins engineered to recognize tumor biomarker mesothelin internalize upon binding. PLoS One 2018; 13(5). e0197029.

[32] Chandler PG, Buckle AM. Development and differentiation in monobodies based on the fibronectin Type 3 domain. Cells 2020;9(3):610.

[33] Pallesen J, Wang N, Corbett KS, Wrapp D, Kirchdoerfer RN, Turner HL, et al. Immunogenicity and structures of a rationally designed prefusion MERS-CoV spike antigen. Proc Natl Acad Sci U S A 2017;114(35):E7348–57.

[34] Stadlbauer D, Amanat F, Chromikova V, Jiang K, Strohmeier S, Arunkumar GA, et al. SARS-CoV-469 2 seroconversion in humans: a detailed protocol for a serological assay, antigen production, and test setup. Curr Protoc Microbiol 2020; 57(1):e100.

[35] Tian X, Li C, Huang A, Xia S, Lu S, Shi Z, et al. Potent binding of 2019 novel coronavirus spike protein by a SARS coronavirus specific human monoclonal antibody. Emerg Microbes Infect 2020;9(1):382–5.

[36] Gorman KT, Roby LC, Giuffre A, Huang R, Kay BK. Tandem phage-display for the identification of non-overlapping binding pairs of recombinant affinity reagents. Nucleic Acids Res 2017;45(18):e158.

[37] Pershad K, Wypisniak K, Kay BK. Directed evolution of the forkhead-associated domain to generate anti-phosphospecific reagents by phage display. J Mol Biol 2012;424(1-2):88–103.

[38] Porath J. Immobilized metal ion affinity chromatography. Protein Expr Purif 1992; 3(4):263–81.

[39] Hewitt SN, Choi R, Kelley A, Crowther GJ, Napuli AJ, et al. Expression of proteins in Escherichia coli as fusions with maltose-binding protein to rescue non-expressed targets in a high-throughput protein expression and purification pipeline. Acta Crystallogr Sect F Struct Biol Cryst Commun 2011;67(Pt 9):1006–9.

[40] Guthe S, Kapinos L, Moglich A, Meier S, Grzesiek S, Kiefhaber T. Very fast folding and association of a trimerization domain from bacteriophage T4 fibritin. J Mol Biol 2004;337(4):905–15.

[41] Birtalan S, Zhang Y, Fellouse FA, Shao L, Schaefer G, Sidhu SS. The intrinsic contributions of tyrosine, serine, glycine and arginine to the affinity and specificity of antibodies. J Mol Biol 2008;377(5):1518–28.

[42] Fellouse FA, Wiesmann C, Sidhu SS. Synthetic antibodies from a four-amino acid code: a dominant role for tyrosine in antigen recognition. Proc Natl Acad Sci U S A 2004;101(34):12467–72.

[43] Fellouse FA, Li B, Compaan DM, Peden AA, Hymowitz SG, Sidhu SS. Molecular recognition by a binary code. J Mol Biol 2005;348(5):1153–62.

[44] Fellouse FA, Esaki K, Birtalan S, Raptis D, Cancasci VJ, Koide A, et al. High-throughput generation of synthetic antibodies from highly functional minimalist phage displayed libraries. J Mol Biol 2007;373(4):924–40.

[45] Wang Y, Liu M, Gao J. Enhanced receptor binding of SARS-CoV-2 through networks of hydrogen-bonding and hydrophobic interactions. Proc Natl Acad Sci U S A 2020;117(25):13967–74.

[46] Wrapp D, Wang N, Corbett KS, Goldsmith JA, Hsieh CL, Abiona O, et al. Cryo-EM structure of the 2019-nCoV spike in the prefusion conformation. Science 2020;367 (6483):1260–3.

[47] Ou J, Zhou Z, Dai R, Zhao S, Wu X, Zhang J, et al. Emergence of SARS-CoV-2 spike RBD mutants that enhance viral infectivity through increased human ACE2 receptor binding affinity. 2020. https://doi.org/10.1101/2020.03.15.991844.

[48] Koide A, Gilbreth RN, Esaki K, Tereshko V, Koide S. High-affinity single-domain binding proteins with a binary-code interface. Proc Natl Acad Sci U S A 2007;104 (16):6632–7.

[49] Barnes CO, Jette CA, Abernathy ME, Dam KA, Esswein SR, Gristick HB, et al. SARS-CoV-2 neutralizing antibody structures inform therapeutic strategies. Nature 2020; 588(7839):682–7.

[50] Zeng X, Li L, Lin J, Li X, Liu B, Kong Y, et al. Isolation of a human monoclonal antibody specific for the receptor binding domain of SARS-CoV-2 using a competitive phage biopanning strategy. Antibody Therap 2020;3(2):95–100.

[51] Huo J, Le Bas A, Ruza RR, Duyvesteyn HME, Mikolajek H, Malinauskas T, et al. Neutralizing nanobodies bind SARS-CoV-2 spike RBD and block interaction with ACE2. Nat Struct Mol Biol 2020;27(9):846–54.

[52] Walter JD, Hutter CAJ, Zimmermann I, Wyss M, Egloff P, Sorgenfrei M, et al. Sybodies targeting the SARS-CoV-2 receptor-binding domain. 2020. https://doi. org/10.1101/2020.04.16.045419.

[53] Piccoli L, Park YJ, Tortorici MA, Czudnochowski N, Walls AC, Beltramello M, et al. Mapping neutralizing and immunodominant sites on the SARS-CoV-2 Spike receptor-binding domain by structure-guided high-resolution serology. Cell 2020; 183(4):1024–42. e21.

[54] Cao L, Goreshnik I, Coventry B, Case JB, Miller L, Kozodoy L, et al. De novo design of picomolar SARS-CoV-2 miniprotein inhibitors. Science 2020;370(6515):426–31.

[55] Tsukiji S, Nagamune T. Sortase-mediated ligation: a gift from Gram-positive bacteria to protein engineering. Chembiochem 2009;10(5):787–98.

[56] Williamson DJ, Fascione MA, Webb ME, Turnbull WB. Efficient N-terminal labeling of proteins by use of sortase. Angew Chem Int Ed Engl 2012;51(37):9377–80.

[57] Zhang Y, Park KY, Suazo KF, Distefano MD. Recent progress in enzymaticprotein labelling techniques and their applications. Chem Soc Rev 2018;47(24):9106–36.

[58] Wyllie AL, Fournier J, Casanovas-Massana A, Campbell M, Tokuyama M, et al. Saliva is more sensitive for SARS-CoV-2 detection in COVID-19 patients than nasopharyngeal swabs. medRxiv 2020.

[59] Perchetti GA, Nalla AK, Huang ML, Zhu H, Wei Y, Stensland L, et al. Validation of SARS-CoV-2 detection across multiple specimen types. J Clin Virol 2020;128: 104438.

[60] Hoogenboom HR. Selecting and screening recombinant antibody libraries. Nat Biotechnol 2005;23(9):1105–16.

[61] Guntas G, Lewis SM, Mulvaney KM, Cloer EW, Tripathy A, Lane TR, et al. Engineering a genetically encoded competitive inhibitor of theKEAP1-NRF2 interaction via structure-based design and 569 phage display. Protein Eng Des Sel 2016;29(1):1–9.

[62] Xiao H, Schultz PG. At the interface of chemical and biological synthesis: an expanded genetic code. Cold Spring Harb Perspect Biol 2016;8(9). a023945.

[63] Li P, Wang L, Di LJ. Applications of protein fragment complementation assay for analyzing biomolecular interactions and biochemical networks in living cells. J Proteome Res 2019;18(8):2987–98.

[64] Konwarh R. Nanobodies: prospects of expanding the gamut of neutralizinh antibodies against the novel coronavirus, SARS-CoV-2. Front Immunol 2020;11: 1531.

[65] Wu Y, Li C, Xia S, Tian X, Kong Y, Wang Z, et al. Identification of human single-domain antibodies against SARS-CoV-2. Cell Host Microbe 2020;27(6):891–8. e5.

[66] Main AL, Harvey TS, Baron M, Boyd J, Campbell ID. The three-dimensional structure of the tenth type III module of fibronectin: an insight into RGD-mediated interactions. Cell 1992;71:671–8.